USGS
science for a changing world

Chronology of Postglacial Eruptive Activity and Calculation of Eruption Probabilities for Medicine Lake Volcano, Northern California

By Manuel Nathenson, Julie M. Donnelly-Nolan, Duane E. Champion, and Jacob B. Lowenstern

Scientific Investigations Report 2007–5174-B

U.S. Department of the Interior
U.S. Geological Survey

U.S. Department of the Interior
DIRK KEMPTHORNE, Secretary

U.S. Geological Survey
Mark D. Myers, Director

U.S. Geological Survey, Reston, Virginia: 2007

This report and any updates to it are available online at:
http://pubs.usgs.gov/sir/2007/5174/b/

For product and ordering information:
World Wide Web: http//www.usgs.gov/pubprod
Telephone: 1-888-ASK-USGS (1-888-275-8747)

For more information on the USGS—the Federal source for science about the Earth,
its natural and living resources, natural hazards, and the environment:
World Wide Web: http://www.usgs.gov
Telephone: 1-888-ASK-USGS (1-888-275-8747)

Suggested citation:
Nathenson, Manuel, Donnelly-Nolan, J.M., Champion, D.E., and Lowenstern, J.B., 2007, Chronology of postglacial eruptive activity and calculation of eruption probabilities for Medicine Lake volcano, northern California: U.S. Geological Survey Scientific Investigations Report 2007-5174-B, 10 p.
[http://pubs.usgs.gov/sir/2007/5174/b/].

Cataloging-in-publication data are on file with the Library of Congress (http://www.loc.gov/).

Produced in the Western Region, Menlo Park, California
Manuscript approved for publication, August 20, 2007
Text edited by Peter Stauffer
Layout and design by Judy Weathers

Contents

Figures

Tables

Chronology of Postglacial Eruptive Activity and Calculation of Eruption Probabilities for Medicine Lake Volcano, Northern California

By Manuel Nathenson, Julie M. Donnelly-Nolan, Duane E. Champion, and Jacob B. Lowenstern

Abstract

Medicine Lake volcano has had 4 eruptive episodes in its postglacial history (since 13,000 years ago) comprising 16 eruptions. Time intervals between events within the episodes are relatively short, whereas time intervals between the episodes are much longer. An updated radiocarbon chronology for these eruptions is presented that uses paleomagnetic data to constrain the choice of calibrated ages. This chronology is used with exponential, Weibull, and mixed-exponential probability distributions to model the data for time intervals between eruptions. The mixed exponential distribution is the best match to the data and provides estimates for the conditional probability of a future eruption given the time since the last eruption. The probability of an eruption at Medicine Lake volcano in the next year from today is 0.00028.

Introduction

Medicine Lake volcano has had four eruptive episodes in its postglacial history (since 13,000 years ago). Time intervals between events within the episodes are relatively short, whereas time intervals between the episodes are much longer (Donnelly-Nolan and others, 1990). To calculate eruption probabilities in such situations, the usual assumption of a Poisson process does not apply, and other models are more appropriate (Nathenson, 2001). Donnelly-Nolan and others (1990) provided a radiocarbon-dated chronology for the postglacial eruptive activity at Medicine Lake volcano, and Nathenson (2001) used this chronology, along with a radiocarbon calibration curve, to estimate eruption probabilities. New data are available subsequent to the chronology of Donnelly-Nolan and others (1990). This refined chronology is presented in the next section, particularly using paleomagnetic data to constrain the choice of calibrated ages from the newer radiocarbon calibration curve of Reimer and others (2004). In addition, the data from a core in Medicine Lake (Starratt and others, 2003) are used to calculate an age for the Medicine Lake Glass Flow. This refined chronology is then used in the second section with several models to estimate the current probability of an eruption at Medicine Lake volcano. That probability provides a basis for the assessment of volcanic hazards at Medicine Lake in Donnelly-Nolan and others (2007).

Chronology

Radiocarbon ages for the postglacial eruptive units of Donnelly-Nolan (in press) are given in table 1. Radiocarbon ages are converted to calibrated (calendar) ages using the calibration curve of Reimer and others (2004) in the calibration program of Stuiver and others (2004). An example of the calibration program's graphical results is given in figure 1 for the weighted mean radiocarbon age for Glass Mountain. The radiocarbon age on the vertical axis is shown with a Gaussian probability distribution for one and two standard deviations (actually standard errors in this case). The probability distribution for the radiocarbon age is then passed through the calibration curve to produce a probability distribution for calibrated calendar ages along the horizontal axis. The spread of the one- and two-sigma uncertainties in the radiocarbon ages are shown in the corresponding shades of gray on the horizontal axis for calendar ages. In table 1, the two-sigma spread in calibrated calendar ages and the ages of the probability maxima are given in the third and fourth columns. For eruptive units with widely separated calibrated ages, the primary maximum in the probability distribution is a reasonable measure of the age—for the example in figure 1, that age would be 780 cal. yr BP. The age range for this chosen age is 790-740 cal. yr BP, though it should be recognized that the age range of 890-870 cal. yr BP is also reasonable at the plus-or-minus-one-sigma level. For eruptive units with widely separated calibrated ages, the probability analysis (see below) is actually not very sensitive to the particular age chosen. However, the paleomagnetic data permit choices to be made between the different probability maxima in the calibrated ages.

Paleomagnetic directions for the eruptive units of table 1 are shown in figure 2. Earth's magnetic north pole and geographic north pole do not commonly coincide. Deriving

Table 1. Radiocarbon ages and calibrated ages for postglacial eruptive units at Medicine Lake volcano.

[Both ^{14}C and calibrated ages are years before present (BP). By convention, present is A.D. 1950. Uncertainties for radiocarbon ages are standard deviations (σ); uncertainties for weighted-mean radiocarbon ages are standard errors. Calibrated ages rounded to nearest 10 years. The calibrated age range gives ages from converting the ^{14}C age plus or minus two standard deviations to calendar years BP. Calibrated ages from the probability distributions are for maxima. Where a range of calibrated age is given, the maximum in the probability distribution is relatively flat. Calibrated ages in parentheses are for secondary maxima in the probability distribution that are sometimes used to satisfy constraints from the paleomagnetic data. Data from Donnelly-Nolan and others (1990), Clynne and others (2002), and this study.]

Sample I.D.	^{14}C age ± 1 σ (BP)	Cal. range ± 2 σ (years BP)	Calibrated age (years BP) from probability	Best cal. age (years BP)
		Episode 4 – (lasts 280 years)		
Rhyolite of Glass Mountain				
1375	865±50	690-910	740-780, (820), (870-890)	
2136	885±40	730-920	740-790, (820), (870-890)	
2652	910±60	700-930	(740), 790, 820, 890	
Wt. Mean	884±28	730-910	740-790, (820),(870-890)	890
Chose secondary maximum oldest age to shorten interval to rhyolite of Little Glass Mountain because of small difference in paleomagnetic pole.				
Rhyolite of Little Glass Mountain				
	1,065±90	780-1,180, 1,210-1,230	940, 960, 1,040	940
Chose youngest age to shorten interval to rhyolite of Glass Mountain because of small difference in paleomagnetic pole and to lengthen interval to Chaos Crags and basaltic andesite of Paint Pot Crater because of significant difference in paleomagnetic poles.				
Lassen Volcanic center: Chaos Crags				
Wt. Mean	1,103±13	970-1,060	980, 1,000, 1,040, 1,050	1,050
Chose oldest age to lengthen interval to rhyolite of Little Glass Mountain because of significant difference in paleomagnetic poles.				
Basaltic andesite of Paint Pot Crater				
				1,110
Because of stratigraphy and small difference in paleomagnetic direction to basaltic andesite of Callahan Flow, chose calendar age as 10 years younger.				
Basaltic andesite of Callahan Flow				
W-5947	1,040±50	800-870, 900-1,060	940, (1,040)	
858	1,110±60	930-1,170	990, 1,030	
2057	1,180±35	980-1,180, 1,210-1,230	1,070, 1,120, 1,160	
Wt. Mean	1,162±30	980-1,170	1,040, 1,060, 1,120, 1,160	1,120
Weighted mean calculated using only two oldest ages, because youngest too discordant (pretreatment issue?). Chose age of 1,120 yr BP because of small difference in paleomagnetic pole to basaltic andesite of Paint Pot Crater and larger difference to paleomagnetic pole of the rhyolite of "Hoffman flows."				
Rhyolite of "Hoffman flows"				
1911	1,190±40	980-1,260	(1,020), 1,070-1,170, (1,220)	
1374	1,220±50	1,010-1,280	1,080-1,170, 1,220	
1373	1,215±40	1,020, 1,060-1,270	1,080-1,170, 1,220	
Wt. Mean	1,207±25	1,060-1,180, 1,210-1,230	1,090-1,170, (1,220)	1,170
Ages from charcoal samples for rhyolite of "Hoffman flows" are from an ash (tephra?) deposit also containing ash from the rhyolite of Glass Mountain. Previously assumed to be discordant ages for the rhyolite of Glass Mountain, they are now proposed as appropriate ages for the rhyolite of "Hoffman flows." Archaeomagnetic record supports a ^{14}C age of 1,200 years. Chose high end of age in range because of difference to paleomagnetic pole for basaltic andesite of Callahan Flow.				
		Episode 3 – (lasts 130 years)		
Andesite of Burnt Lava Flow				
2711	2,820±40	2,800-2,820, 2,840-3,060	2,880-2,950, (3,010-3,060)	2,950
2712	2,715±40	2,750-2,880, 2,910-2,920	2,780-2,840, (2,910)	
Wt. Mean	2,768±28	2,790-2,950	(2,800-2,820), 2,860, (2,915), (2,940)	
Sample 2712 is from bark and may be too young. Chose oldest age of primary maximum for sample 2711 to shorten interval to basalt of Black Crater and Ross Chimneys because of moderate difference in paleomagnetic poles.				
Basalt of Black Crater and Ross Chimneys				
2766	3,025±45	3,080-3,360	(3,080), 3,170, 3,220-3,250, 3,310	3,080
Chose secondary maximum youngest age to shorten interval to andesite of Burnt Lava Flow because of moderate difference in paleomagnetic poles.				

Table 1. Radiocarbon ages and calibrated ages for postglacial eruptive units at Medicine Lake volcano.—Continued

[Both ^{14}C and calibrated ages are years before present (BP). By convention, present is A.D. 1950. Uncertainties for radiocarbon ages are standard deviations (σ); uncertainties for weighted-mean radiocarbon ages are standard errors. Calibrated ages rounded to nearest 10 years. The calibrated age range gives ages from converting the ^{14}C age plus or minus two standard deviations to calendar years BP. Calibrated ages from the probability distributions are for maxima. Where a range of calibrated age is given, the maximum in the probability distribution is relatively flat. Calibrated ages in parentheses are for secondary maxima in the probability distribution that are sometimes used to satisfy constraints from the paleomagnetic data. Data from Donnelly-Nolan and others (1990), Clynne and others (2002), and this study.]

Sample I.D.	^{14}C age ± 1 σ (BP)	Cal. range ± 2 σ (years BP)	Calibrated Age (years BP) from probability	Best Cal. Age (years BP)
		Episode 2 – (lasts 100 years)		
Dacite of pit craters				
2649	4,430±70	4,860-5,290	4,980-5,000, 5,040, 5,210	5,040
2709	4,280±40	4,710-4,750, 4,820-4,970	4,850	
Wt. Mean	4,317±35	4,840-4,970	4,860, (4,940)	
Because of small difference in paleomagnetic poles with dacite of Medicine Lake Glass Flow, calendar ages for sample 2709 are too young. It is therefore assumed that sample 2649 is more representative of correct age, and its middle calibrated age is picked as representative.				
Dacite of Medicine Lake Glass Flow				
Core B100NC-1				5,140
Age from Medicine Lake Core B100NC-1(see text). Equivalent ^{14}C age is 4,510 years BP.				
		Episode 1 – (lasts 230 years, including precursors to basalt of Giant Crater)		
Basalt of Valentine Cave				
2651	10,850±60	12,800-12,920	12,850	12,260
Because of small difference with paleomagnetic pole for basalt of "vent 5," a time interval of 10 years is chosen. ^{14}C date presumed too old because of younger dates for older events.				
Basalt of "vent 5"				
2701	10,355±50	12,000-12,400, 12,520-12,600	12,100-12,220, (12,270),12,330	12,270
Oldest age is slightly older than basalt of Devils Homestead, so chose secondary maximum that is younger but not too much younger than basalt of Devils Homestead because of not very large difference in paleomagnetic poles.				
Basalt of Devils Homestead				12,320
Age assumed to be 10 years before basalt of tree molds because of very similar paleomagnetic direction.				
Basalt of tree molds				
2053	10,200±110	11,400-12,400	11,830, 11,970, (12,330)	12,330
Chose secondary mode oldest age to shorten interval to basalt of Giant Crater because of small difference in paleomagnetic poles.				
Basalt of Giant Crater				
1904A	10,580±80	12,240-12,270, 12,360-12,820	12,430, 12,670	
1904B	10,620±80	12,400-12,820	12,400, 12,700	
Wt. Mean	10,600±57	12,400-12,520, 12,560-12,800	12,430, 12,680	12,430
Taken as starting point for chronology of Episode 1. Chose younger age so that basalt of ribbon flows can have older age.				
		Precursors to basalt of Giant Crater		
Basalt of ribbon flows				
2700	10,310±60	11,830-11,910, 11,950-12,390	12,080, 12,220, (12,330), (12,480-12,560)	12,480
Chose age near secondary maximum oldest age so that age is older than but close to basalt of Giant Crater because of small difference in paleomagnetic poles.				
Basaltic andesite east of Grasshopper Flat				
2650	10,930±50	12,830-12,950	12,880	
A-2650	10,690±70	12,410-12,450, 12,610-12,850	(12,430), 12,730, 12,790	12,490
Chose younger age on slope of secondary maximum for sample A-2650 so that intervals to basalt of ribbon flows and basalt of Giant Crater are short because of small differences in paleomagnetic poles. Assumed that age for sample 2650 is too old because of small differences in paleomagnetic poles.				

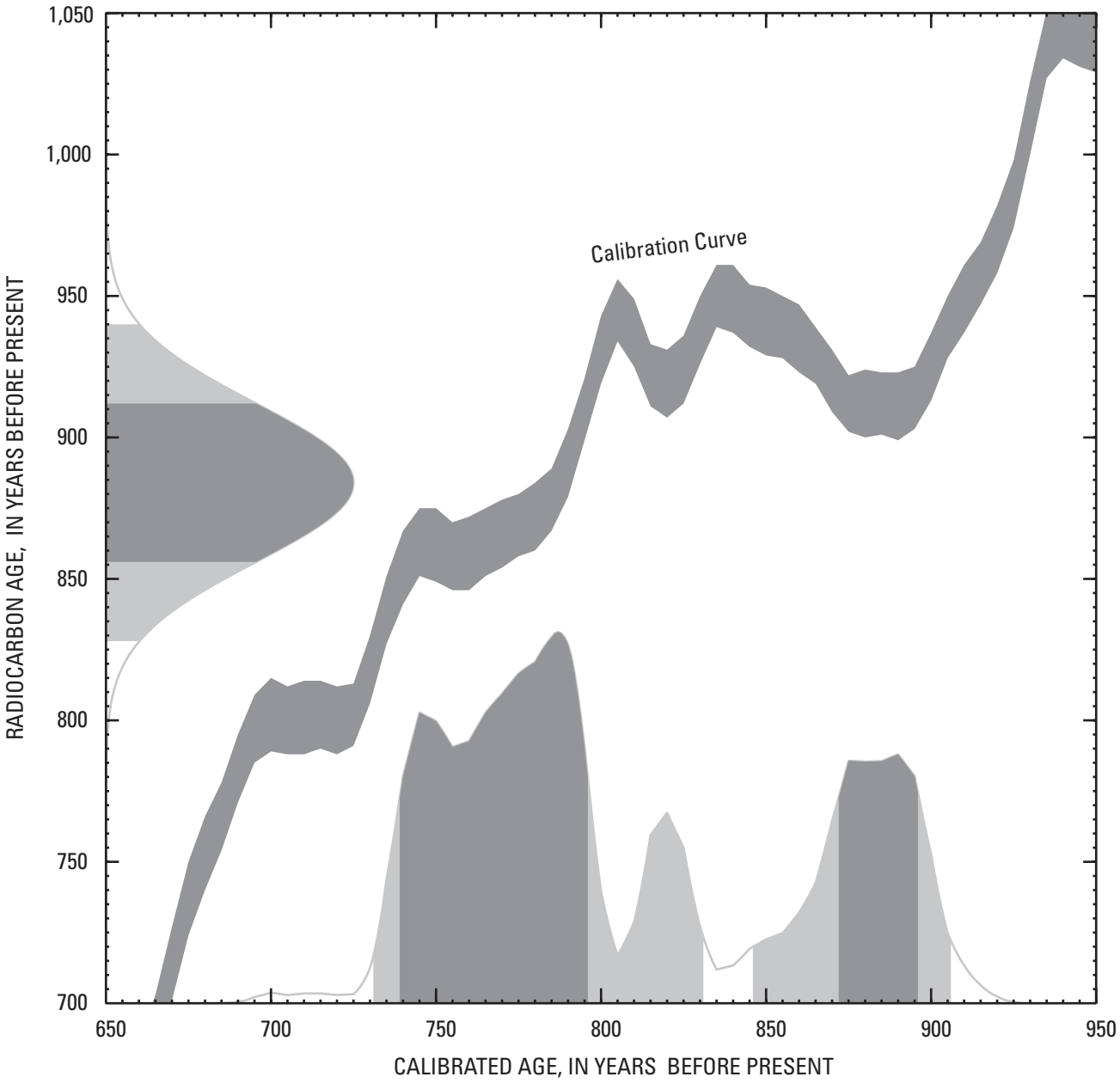

Figure 1. Radiocarbon calibration curve from Reimer and others (2004) for weighted mean age of rhyolite of Little Glass Mountain. Normal law of error (more properly probability density function for the normal distribution) for radiocarbon age of 884±28 yr shown along y-axis. Mean and plus and minus one (dark grey) and two (light grey) standard deviations for radiocarbon age shown. Scale not shown for values of probability. Calibration curve in the middle shows correspondence between radiocarbon ages (y-axis) and calibrated ages (x-axis) along with the uncertainty in the calibration (shown by thickness of curve). A single radiocarbon age can have multiple values of calibrated age. Probability density function for calibrated age shown along x-axis calculated with the computer program of Stuiver and others (2004). Multiple values of calibrated age for a single radiocarbon age result in the single-peaked probability density function shown on the y-axis becoming a multiply peaked probability density function along the x-axis.

paleomagnetic directions involves determining both the declination (compass direction) and the inclination (angle from the horizontal). The direction of the Earth's magnetic field at a given location changes with time in response to internal Earth processes, yielding movement known as secular variation. Lava flows record the direction of the magnetic field at the time the lava cools through the Curie temperature and the direction becomes fixed. The paleomagnetic directions in figure 2 are based on sampling each unit at one or more sites with multiple cores drilled at each site. Each core is oriented using a sun compass, and the direction of magnetization is subsequently measured in the laboratory. Sampling sites were carefully selected to avoid areas of post-magnetization rotation or deformation of the flows.

Paleomagnetic secular variation in the western United States has been recently documented by Hagstrum and Champion (2002). The rate at which paleomagnetic direction changes is not constant, but the relative positions of the directions in figure 2 provide some significant constraints on the likely time between events. For directions that are nearly coincident, such as those for the Paint Pot Crater flow and the Callahan Flow, there is likely to be only a few to perhaps as many as 50 years between the times of the flows. We use 10 years for the time interval between the Paint Pot Crater flow and the Callahan Flow. For a somewhat larger spread between the paleomagnetic directions, we assume that the likely time difference is 50 years, though it could be as much as 100 years. For the interval between Glass Mountain and Little Glass Mountain, we choose calibrated ages that are separated by 50 years. For a larger spread in broadly similar paleomagnetic directions, we assume that the likely time difference is 100 years. For the interval between Little Glass Mountain and

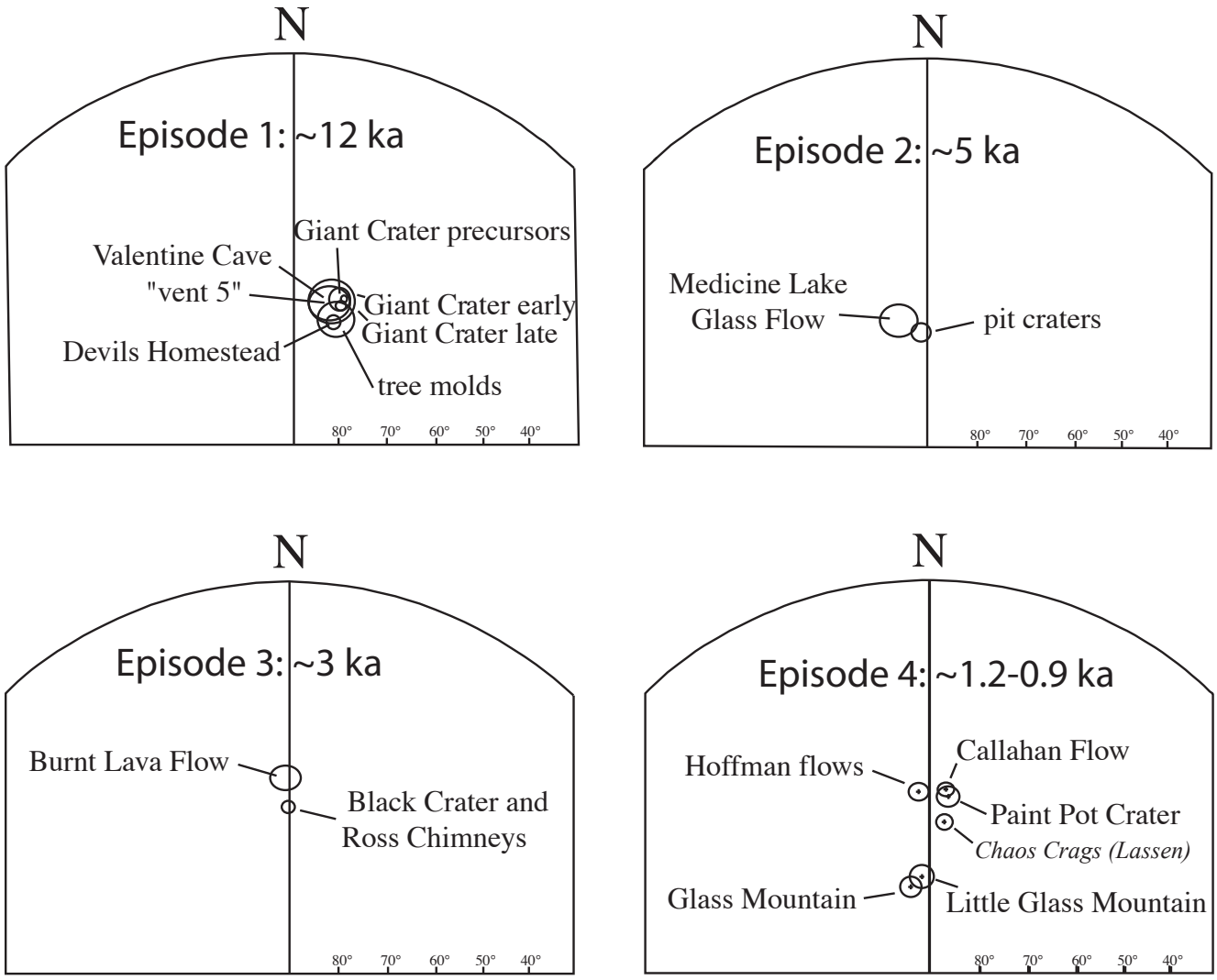

Figure 2. Paleomagnetic directions of magnetization for postglacial eruptive units of Medicine Lake volcano listed in table 1, shown on a lower hemisphere equal-area projection. The inclination scale is shown, and the declination angle starts from zero degrees along the arc at north running clockwise. Circles and ellipses represent 95-percent confidence limits for each mean direction.

the Chaos Crags eruptive unit at Lassen Volcanic National Park, which show a significant difference in paleomagnetic direction, we pick the youngest and oldest calibrated ages to maximize the time interval separating the units at 110 years.

The choices made for calibrated ages based on the paleomagnetic data are given in table 1. In developing the chronology for episode 1, we chose the age of the Giant Crater flow as the starting point and applied paleomagnetic data to choose calibrated ages for the units younger and older in time. The calibrated age of the Valentine Cave flow simply does not fit the paleomagnetic data, probably because the dated charcoal represents only a minuscule sample from a tree mold of a meter-sized tree that could have been a thousand years old. We therefore chose an age for the Valentine Cave flow based on the small difference with the paleomagnetic direction for the "vent 5" event.

Based on the combination of paleomagnetic and radiocarbon data, the chronologies for episodes 1 and 4 result in durations of 230 and 280 years, respectively. Episode 4 has a larger spread in paleomagnetic directions than episode 1 (fig. 2) and only slightly greater duration than episode 1. This may indicate that the rate of secular variation was faster during episode 4 than during episode 1, or it may be an artifact of the uncertainty in the radiocarbon dates.

The age of the Medicine Lake Glass Flow is obtained from the data for Core B100NC-1 for Medicine Lake (Starratt and others, 2003). The data for this core include several radiocarbon ages for organic mats (table 2). Three tephra layers have been correlated to eruptions from Medicine Lake volcano (table 2) on the basis of petrographic examination and electron microprobe chemical analyses by Jacob Lowenstern (unpublished data, 2003). Combining the calibrated ages for the known tephra layers with the calibrated ages for the organic mats, the sedimentation rate shown in figure 3 is obtained. The estimated calibrated age for the Medicine Lake Glass Flow is 5,140 cal. yr BP (5,135 cal. yr BP unrounded), and the back-calculated radiocarbon age would be 4,510 yr BP. The correlation shown in figure 3 uses the single estimated age for each volcanic layer or organic mat. The same correlation has been done using the multiple calibrated ages in table 2, and the resulting age for the Medicine Glass Flow is 5,130 cal. yr BP (5,132 cal. yr BP unrounded), not significantly different from the estimate using single calibrated ages.

The best calibrated ages presented in table 1 are estimates based on combining calibrated ages and paleomagnetic constraints. It is important to recognize that there are still significant uncertainties in the chosen ages. A time interval that was chosen as 10 years could be 1, 20, or even 50 years, with similar uncertainties for all intervals. The age of an episode could be off by 50 or even 100 years. But the overall pattern of episodes of relatively short duration (100-300 years) with an average time between eruptions of only 62 years, separated by long periods with no activity (1,780, 1,960, and 7,120 years) will not change with the kind of revisions that are likely to occur as better constraints on the timing of eruptions are developed from refined data. This characteristic of disparate eruption time intervals is fundamentally important for the probability analysis in the next section.

Probabilities

An underlying assumption of U.S. Geological Survey volcano hazards assessments for Cascade volcanoes in Oregon and Washington has been that the probability distribution of time intervals between volcanic eruptions may be treated as a Poisson process. Time histories for some volcanoes match this assumption well (for example, Klein, 1982). The probability of an eruption during any particular period of time is calculated from the relation for the occurrence rate. For a Poisson process, this relation is obtained from the exponential distribution for the probability $P\{ T \le t\}$ that an eruption will occur in a time T less than or equal to the time period t:

$$P\{ T \le t\} = F(t) = 1 - e^{-\mu t}$$
$$\approx \mu t \text{ , for } \mu t \text{ small,}$$

where $F(t)$ is the symbol for the probability distribution function, and μ is the mean occurrence rate (events per year) for the exponential distribution. Because occurrence rates are low in the Cascades, the approximate relation shown above is normally used (for example, Scott and others, 1995).

Given a set of n eruption time intervals t_i, the average recurrence interval (the reciprocal of the occurrence rate) may be determined by:

$$\frac{1}{\mu} = \frac{1}{n} \sum_{i=1}^{n} t_i \ .$$

The properties of a Poisson process include the characteristic that the conditional probability of an eruption occurring within a time period does not depend on the time already waited but only on the time period selected (for example, 1 year, 30 years, or 100 years) to calculate a conditional probability. For some volcanoes, the time history contains disparate time intervals between eruptions, some being short and others much longer. Some examples of time histories having such disparate eruption-time intervals are those of Mount Rainier and Mount St. Helens in Washington. Mullineaux's (1974) data for eruption times of tephra layers at Mount Rainier have three long intervals (>2,000 years) and seven short intervals (<600 years) between eruptions. Mullineaux's (1996) data for Mount St. Helens include 1 interval of 8,600 years, 1 of 1,500 years, and 34 of less than 640 years. In such instances, other probability distributions more accurately represent the data, and the conditional probabilities based on those distributions do depend on the time since the last eruption.

Bebbington and Lai (1996) proposed using the Weibull distribution to model eruption times that vary with the preceding time interval:

$$P\{ T \le t\} = F(t) = 1 - e^{-\mu(t)}$$
$$\text{where } \mu(t) = \left(\frac{t}{\theta}\right)^{\beta}$$

and T is the time, less than the time period t, to the next eruption. Parameters θ and β are referred to as the scale and shape parameters, respectively; when $\beta = 1$, this reduces to the exponential distribution.

For eruption intervals that can be divided into two populations, one with short intervals and one with long intervals, a model that includes this behavior is the mixed exponential (Cox and Lewis, 1966; Nathenson, 2001):

$$P\{ T \le t\} = F(t) = 1 - p_1 \, e^{-\mu_1 t} - p_2 \, e^{-\mu_2 t}$$

$$\text{where } p_1 = \frac{n_1}{n_1 + n_2}$$

$$\text{and } \frac{1}{\mu_1} = \frac{1}{n_1} \sum_{i=1}^{n_1} t_i$$

where p_1 is the fraction of short intervals, μ_1 is the average occurrence rate for the short intervals, n_1 is the number of short intervals. and p_2, μ_2, n_2 are equivalent parameters for the long intervals. The basic notion embodied in the mixed exponential is that there are two states, one involving short intervals and a second involving long intervals. The probability of an eruption occurring in each of these states is governed by an exponential distribution. If one knows that the volcano is currently in a particular state (a difficult judgment to make), then the probability of an eruption can be calculated using the appropriate exponential relation for that state only.

The probability of direct interest is the conditional probability $P\{\Delta t \le T \le t + \Delta t \mid T > \Delta t\}$ of an eruption occurring between time Δt and time $t + \Delta t$ (for example, during the next year or the next 30 years), after already waiting a time Δt since the last eruption. It can be shown that this conditional probability can be calculated from the distribution function $F(t)$ as

$$P\{\Delta t \le T \le t + \Delta t \mid T > \Delta t\} = 1 - \frac{1 - F(t + \Delta t)}{1 - F(\Delta t)}.$$

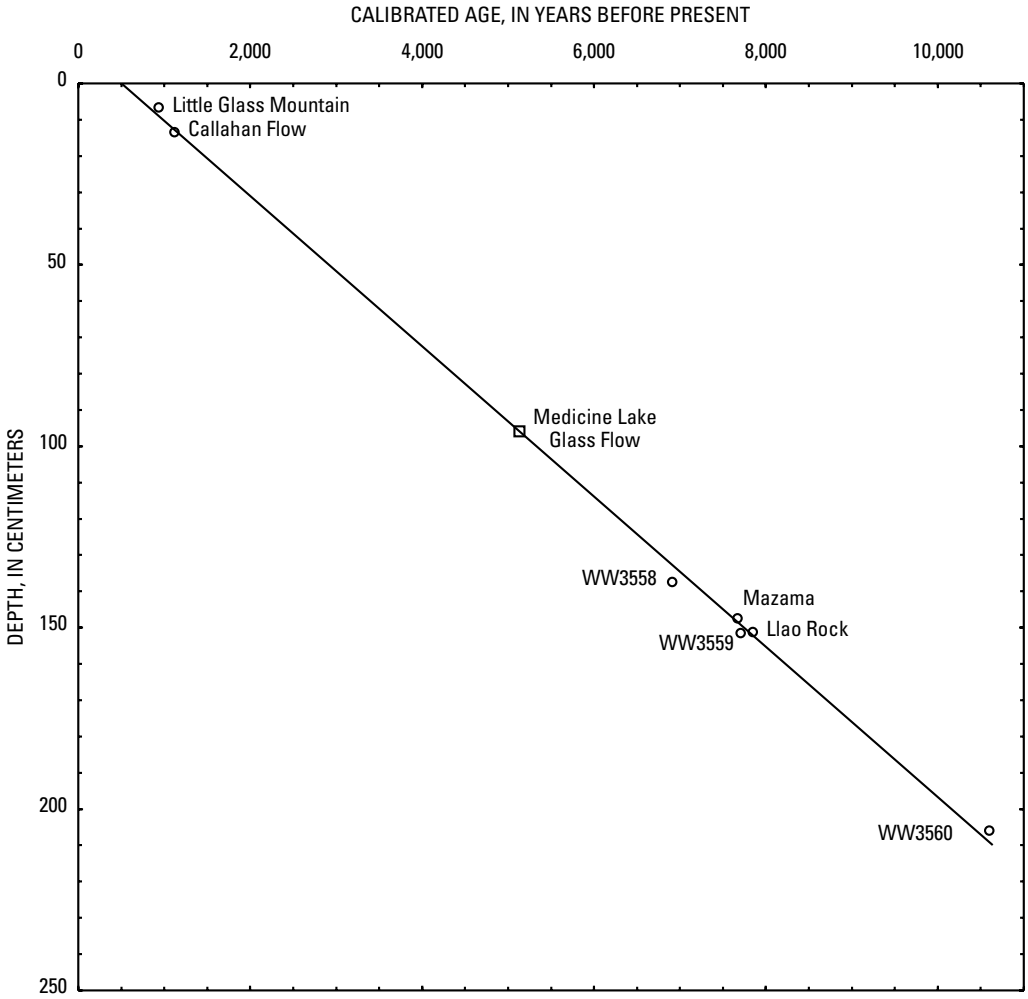

Figure 3. Age-depth relation for Core B100NC-1 from Medicine Lake. The calibrated radiocarbon ages in table 2 (circles) are used to determine the age of the Medicine Lake Glass Flow (square).

For the simple exponential distribution, the conditional probability reduces to:

$$P\{\Delta t \le T \le t + \Delta t \mid T > \Delta t\} = 1 - e^{-\mu t}.$$

Thus, for the simple exponential distribution, the passage of past time does not change the probability of the time to a future eruption. (In the engineering language of time to failure, there is no wear or fatigue). For the Weibull distribution, the conditional probability is:

$$P\{\Delta t \le T \le t + \Delta t \mid T > \Delta t\} = 1 - \exp\left\{\left(\frac{\Delta t}{\theta}\right)^{\beta} - \left(\frac{t+\Delta t}{\theta}\right)^{\beta}\right\}.$$

For the mixed exponential, the conditional probability is:

$$P\{\Delta t \le T \le t + \Delta t \mid T > \Delta t\} = 1 - \left[p_1 e^{-\mu_1 (t+\Delta t)} + p_2 e^{-\mu_2 (t+\Delta t)}\right] / \left[p_1 e^{-\mu_1 \Delta t} + p_2 e^{-\mu_2 \Delta t}\right].$$

Thus, in contrast to the simple exponential distribution, the conditional probability for the mixed exponential does depend on the time since the last eruption, Δt.

Time intervals between postglacial eruptions for Medicine Lake volcano are calculated from the eruption chronology in table 1. The time intervals are ordered and used to calculate the probability distribution for the data, as shown in figure 4 along with the three probability models. Most of the time intervals between eruptions are relatively short, but three are long intervals. The mixed exponential is the best fit to the data (fig. 4) and is able to provide a good match to the disparate eruption time intervals. The conditional probability of an eruption occurring in the next year is given in figure 5 for each of the three distributions. The line marked today represents 947 years since the last eruption (890 cal. yr BP plus 57 years since 1950 to 2007). The probability of an eruption in the next year from today is 0.00028 for the mixed exponential, 0.0013 for the exponential, and 0.0011 for the Weibull distribution. In the year following an eruption, the probability of an eruption in the next year is 0.013 for the mixed exponential, 0.0013 for the exponential, and 0.051 for the Weibull (off the scale of figure 5). Higher probabilities immediately following an eruption are what one would expect intuitively. The constant probability of the simple exponential is an underestimate shortly after an eruption and an overestimate a long time after an eruption. Based on its better agreement with the data in figure 4, the probability estimates from the mixed exponential are proposed as the best estimate for the current eruption probability, that is 0.00028 in the next year.

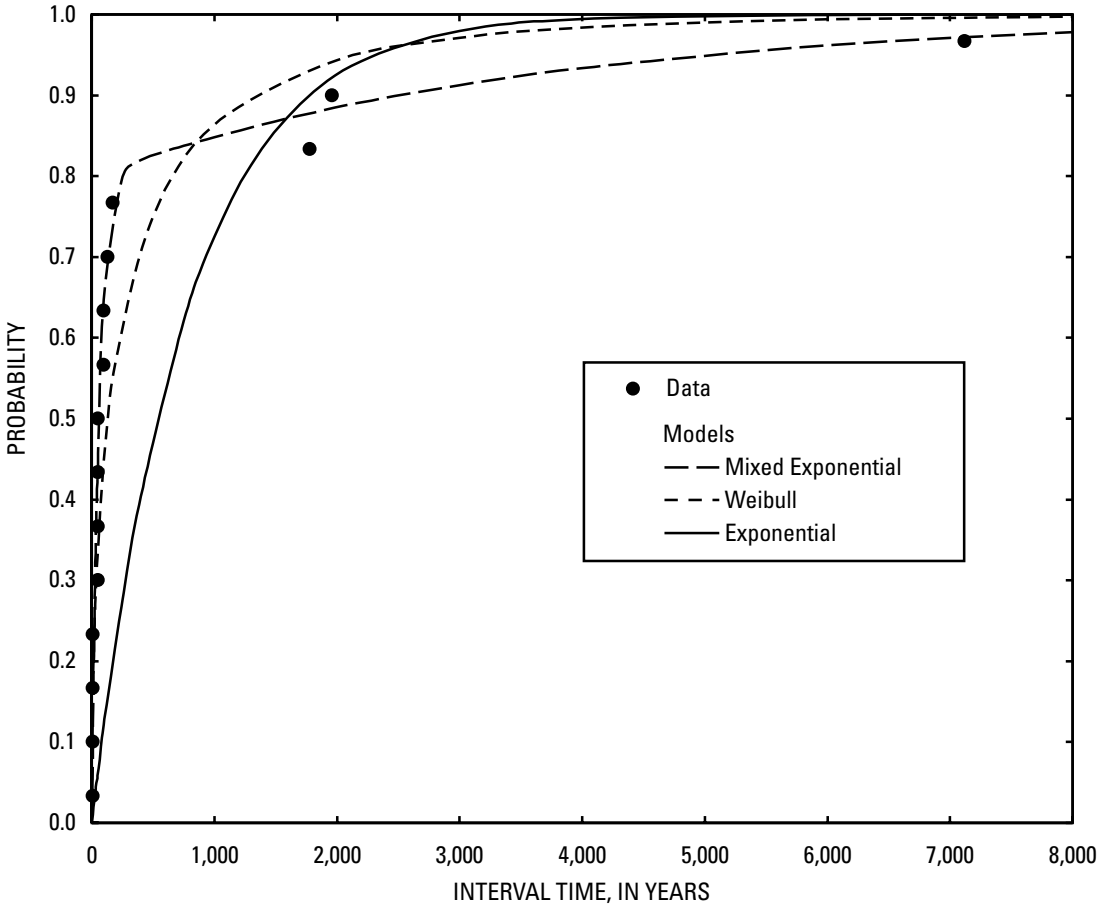

Figure 4. Probability that an eruption will occur in a time less than a given time interval between eruptions. Data from table 1 used to calculate time intervals between postglacial eruptions at Medicine Lake shown as circles, along with curves representing three models for the data. The mixed-exponential distribution is the closest match to the data.

Table 2. Radiocarbon and calibrated ages for Core B100NC-1 from Medicine Lake (Starratt and others, 2003) for ashes and organic mats (WW samples).

[Ashes from eruptions identified using SEM images and microprobe chemistry by Lowenstern (unpublished data, 2003). Uncertainties for radiocarbon ages are standard deviations (σ); uncertainties for weighted-mean radiocarbon ages are standard errors. Calibrated ages rounded to nearest 10 years. The calibrated age range gives ages from converting the radiocarbon age plus or minus two standard deviations to calendar years BP. Calibrated ages from the probability distributions are for maxima. Data from table 1, Starratt and others (2003), and Bacon (1983). Best ages in cal. yr BP from table 1 and chosen on the basis of maximum in probability distribution for additional ages in the table.]

Sample I.D.	^{14}C age ± 1 σ (BP)	Cal. range ± 2 σ years (BP)	Calibrated age (years BP) from probability	Best cal. age (years BP)	Depth in core (cm)
Rhyolite of Little Glass Mountain					
	1,065±90	780-1,180, 1,210-1,230	940, 1,040	940	6.75
Basaltic andesite of Callahan Flow					
Wt. Mean	1,162±30	980-1,170	1,040, 1,060, 1,120, 1,160	1,120	13.5
Dacite of Medicine Lake Glass Flow					
Core B100NC-1				5,140	96
[Age from Medicine Lake Core B100NC-1 (see text). Equivalent ^{14}C age is 4,510 years BP.]					
WW3558	6,060±40	6,790-7,140	6,900, 6,930	6,910	137.5
Mazama					
Wt. Mean	6,845±50	7,590-7,790	7,670	7,670	147.5
Llao Rock					
USGS-870	7,015±45	7,740-7,950	7,850, 7,910	7,850	151.25
WW3559	6,910±40	7,670-7,830	7,700, 7,720, 7,780	7,710	151.5
WW3560	9,400±40	10,520-10,730	10,590, 10,650	10,600	206

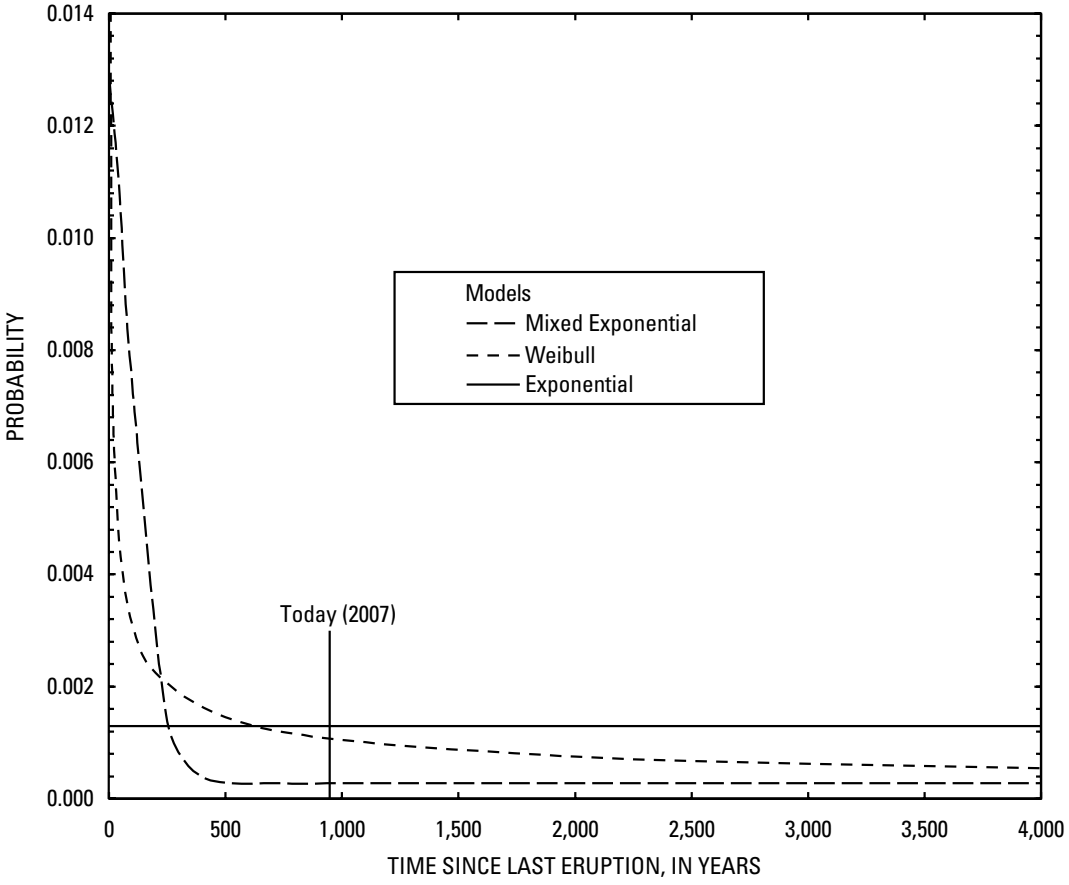

Figure 5. Conditional probability that an eruption will occur at Medicine Lake volcano in the next year, given a time since the last eruption. The line marked today is for 947 years since the last eruption (890 cal. yr BP plus 57 years since 1950 to 2007). The probability estimates from the mixed-exponential distribution are proposed as the best estimate for the current eruption probability, because they agree better with the data in figure 4. The probability of an eruption in the next year is 0.00028 for the mixed exponential. In the year following an eruption, the probability of an eruption in the next year is 0.013 for the mixed exponential.

References Cited

Bacon, C.R., 1983, Eruptive history of Mount Mazama and Crater Lake caldera, Cascade Range, U.S.A.: Journal of Volcanology and Geothermal Research, v. 18, p. 57-115.

Bebbington, M.S., and Lai, C.D., 1996, On nonhomogeneous models for volcanic eruptions: Mathematical Geology, v. 28, p. 585-600.

Clynne, M.A., Christiansen, R.L., Trimble, D.A., and McGeehin, J.P., 2002, Radiocarbon dates from volcanic deposits of the Chaos Crags and Cinder Cone eruptive sequences and other deposits, Lassen Volcanic National Park and vicinity, California: U.S. Geological Survey Open-File Report 02-290, 21 p.

Cox, D.R., and Lewis, P.A.W., 1966, The statistical analysis of series of events: London, Methuen, 285 p.

Donnelly-Nolan, J.M., in press, Geologic map of Medicine Lake volcano, northern California: U.S. Geological Survey Scientific Investigations Map 2927, scale 1:50,000.

Donnelly-Nolan, J.M., Champion, D.E., Miller, C.D., Grove, T.L., and Trimble, D.A., 1990, Post-11,000-year volcanism at Medicine Lake volcano, Cascade Range, northern California: Journal of Geophysical Research, v. 95, p. 19693-19704.

Donnelly-Nolan, J.M., Nathenson, Manuel, Champion, D.E., Ramsey, D.W., Lowenstern, J.B., and Ewert, J.W., 2007, Volcano hazards assessment for Medicine Lake volcano, northern California: U.S. Geological Survey Scientific Investigations Report 2007-5174-A, 26 p., 1 plate [http://pubs.usgs.gov/sir/2007/5174/a/].

Hagstrum, J.T., and Champion, D.E., 2002, A Holocene paleosecular variation record from ^{14}C-dated volcanic rocks in western North America: Journal of Geophysical Research, v. 107, no. B1, 10.1029/2001JB000524, 14 p.

Klein, F.W., 1982, Patterns of historical eruptions at Hawaiian volcanoes: Journal of Volcanology and Geothermal Research, v. 12, p. 1-35.

Mullineaux, D.R., 1974, Pumice and other pyroclastic deposits in Mount Rainier National Park, Washington: U.S. Geological Survey Bulletin 1326, 83 p.

Mullineaux, D.R., 1996, Pre-1980 tephra-fall deposits erupted from Mount St. Helens, Washington: U.S. Geological Survey Professional Paper 1563, 99 p.

Nathenson, Manuel, 2001, Probabilities of volcanic eruptions and application to the recent history of Medicine Lake Volcano, *in* Vecchia, A.V., comp., A unified approach to probabilistic risk assessments for earthquakes, floods, landslides, and volcanoes, November 16-17, 1999, Golden, Colorado: U.S. Geological Survey Open-File Report 01-324, p. 71-74.

Reimer, P.J., Baillie, M.G.L., Bard, Edouard, Bayliss, Alex, Beck, J.W., Bertrand, C.J.H., Blackwell, P.G., Buck, C.E., Burr, G.S., Cutler, K.B., Damon, P.E., Edwards, R.L., Fairbanks, R.G., Friedrich, Michael, Guilderson, T.P., Hogg, A.G., Hughen, K.A., Kromer, Bernd, McCormac, Gerry, Manning, Sturt, Bronk Ramsey, C., Reimer, R.W., Remmele, Sabine, Southon, J.R., Stuiver, Minze, Talamo, Sahra, Taylor, F.W., van der Plicht, Johannes, and Weyhenmeyer, C.E., 2004, INTCAL04 terrestrial radiocarbon age calibration, 0-26 cal kyr BP: Radiocarbon, v. 46, p. 1029-1058.

Scott, W.E., Iverson, R.M., Vallance, J.W., and Hildreth, Wes, 1995, Volcano hazards in the Mount Adams region, Washington: U.S. Geological Survey Open-File Report 95-492, 11 p., 2 plates, scale 1:500,000, 1:100,000.

Starratt, S.W., Barron, J.A., Kneeshaw, Tara, Phillips, R.L., Bischoff, J.L., Lowenstern, J.B., and Wanket, J.A., 2003, A Holocene record from Medicine Lake, Siskiyou County, California; preliminary diatom, pollen, geochemical, and sedimentological data, *in* West, G.J., and Blomquist, N.L., eds., Proceedings of the Nineteenth Annual Pacific Climate Workshop: Interagency Ecological Program for the San Francisco Estuary Technical Report 71, p. 131-148.

Stuiver, Minze, Reimer, P.J., and Reimer, Ron, 2004, CALIB 5.0: Quaternary Isotope Laboratory, University of Washington [http://calib.qub.ac.uk/].